^{103}Rh Chemical Shifts in Complexes Bearing Chelating Bidentate Phosphine Ligands

Walter Leitner,*,† Michael Bühl,*,‡ Roland Fornika,|| Christian Six,† Wolfgang Baumann,§ Eckhard Dinjus,|| Magnus Kessler,† Carl Krüger,† and Anna Rufińska†

Max-Planck-Institut für Kohlenforschung, Kaiser-Wilhelm-Platz 1, 45470 Mülheim/Ruhr, Germany, Organisch-chemisches Institut, Universität Zürich, Winterthurestrasse 190, 8057 Zürich, Switzerland, Institut für Organische Katalyseforschung an der Universität Rostock, Arbeitsgruppe "Komplexkatalyse", Rostock, Germany, and Forschungszentrum Karlsruhe, Technik und Umwelt, Institut für Technische Chemie, Karlsruhe, Germany

Received December 3, 1998

Experimental and theoretical methods have been employed to investigate the influence of the chelating phosphine ligand on the ^{103}Rh chemical shift in complexes containing the [(P$_2$)Rh] fragment (P$_2$ = chelating bidentate phosphine). The δ(^{103}Rh) values obtained by 2D(^{31}P,^{103}Rh{^{1}H}) NMR spectroscopy for a series of neutral rhodium complexes [{R$_2$P(CH$_2$)$_n$-PR$_2$}Rh(hfacac)] (R = Ar, Ph, Cy, Me, n = 1−4, hfacac = hexafluoroacetylacetonate) have been compared. Systematic variation of the phosphine ligand has allowed separation of electronic and geometrical effects. The purely electronic influence of *para* substituents in complexes [{(*p*-XC$_6$H$_4$)$_2$P(CH$_2$)$_4$P(*p*-XC$_6$H$_4$)$_2$}Rh(hfacac)] correlates directly with the Hammett σ_p constants of X, but leads to variations in the chemical shift of less than 80 ppm between X = CF$_3$ and X = OMe. In contrast, geometrical changes in complexes [(P$_2$)Rh(hfacac)] lead to variations in the chemical shift over a range of approximately 800 ppm. The individual contributions of various structural parameters on the δ(^{103}Rh) values have been assessed by density-functional-based calculations for suitable model compounds. The same approach has been extended to the rationalization of the trends in ^{103}Rh chemical shifts of cationic complexes with four P donor ligands around a Rh(+I) center and selected anionic Rh(−I) complexes [(P$_2$)$_2$Rh]$^-$. This analysis allows for the first time a direct corroboration of geometrical variations and their effect on ^{103}Rh chemical shifts, demonstrating that correlations of reactivity with ^{103}Rh chemical shifts can give valuable information on structure/reactivity relationships.

Introduction

The fragment [(P$_2$)Rh] (P$_2$ = chelating bidentate phosphine of general formula R$_2$P−(X)−PR$_2$) plays a crucial role in a plethora of catalytic reactions. The controlling influence of the chelating phosphine ligand on the activity and the selectivity of such transformations is well documented.[1] A number of attempts have been made to develop "ligand parameters"[2] that relate these ligand effects[3] to either structural (e.g., steric bulk, bite angle) or electronic (e.g., basicity) properties. Despite the practical value of such distinctions in catalyst development,[4,5] both structural and electronic param-

† Max-Planck-Institut für Kohlenforschung.
‡ Organisch-chemisches Institut.
§ Institut für Organische Katalyseforschung an der Universität Rostock.
|| Forschungszentrum Karlsruhe.

(1) (a) *Comprehensive Organometallic Chemistry*; Abel, E. W., Stone, F. G. A., Wilkinson, G., Eds.; Pergamon Press: Oxford, 1995; Vol. 12. (b) Crabtree, R. H. *The Organometallic Chemistry of the Transition Metals*; Wiley: New York, 1994. (c) *Homogeneous Transition Metal Catalyzed Reactions*; Moser, W. R., Slocum, D. W., Eds.; Adv. Chem. Ser. 230; 1992. (d) *Applied Homogeneous Catalysis with Organometallic Compounds*; Cornils, B., Herrmann, W. A., Eds.; VCH: Weinheim, 1996.

(2) For a classical textbook example: Tolman, C. A. *Chem. Rev.* **1977**, *77*, 312. For more recent discussions: Brown, T. L. *Inorg. Chem.* **1995**, *34*, 2718. Drago, R. S.; Joerg, S. *J. Am. Chem. Soc.* **1996**, *118*, 2654. Fernandez, A.; Reyes, C.; Wilson, M. R.; Woska, D. C.; Prock, A.; Giering, W. P. *Organometallics* **1997**, *16*, 342. Joerg, S.; Drago, R. S.; Sales, J. *Organometallics* **1998**, *17*, 589.

(3) We restrict our discussion to *intrinsic* ligand effects, i.e., direct effects of ligands on metal centers of catalytically active intermediates. In a practical catalytic system, however, other possibilities must also be taken into account, e.g., formation of different active intermediates, partial dissociation, etc. For example see: (a) Graf, E.; Leitner, W. *Chem. Ber.* **1996**, *129*, 91. (b) Portnoy, M.; Milstein, D. *Organometallics* **1993**, *12*, 1655. (c) Shaw, B. L.; Perera, S. D. *Chem. Commun.* **1998**, 1863.

(4) For mainly geometric variations see: (a) Casey, C. P.; Whiteker, G. T.; Melville, M. G.; Petrovich, L. M.; Gavney, J. A., Jr.; Powell, D. R. *J. Am. Chem. Soc.* **1992**, *114*, 5535. (b) Kranenburg, M.; van der Burgt, Y. E. M.; Kramer, P. C. J.; van Leeuwen, P. W. N. M.; Goubike, K.; Fraanje, J. *Organometallics* **1995**, *14*, 3081. (c) Hofmann, P.; Meier, C.; Hiller, W.; Hickel, M.; Riede, J.; Schmidt, M. U. *J. Organomet. Chem.* **1995**, *490*, 51.

(5) For mainly electronic variations see: (a) Jacobsen, E. J.; Zhang, W.; Güler, M. L. *J. Am. Chem. Soc.* **1991**, *113*, 6703. (b) RajanBabu, T. V.; Ayers, T. A.; Casalnuovo, A. L. *J. Am. Chem. Soc.* **1994**, *116*, 4101. (c) Casalnuovo, A. L.; RajanBabu, T. V.; Ayers, T. A.; Warren, T. H. *J. Am. Chem. Soc.* 9869. (d) Chan, A. S. C.; Pai, C.-C.; Yang, T.-K.; Chen, S.-M. *J. Chem. Soc., Chem. Commun.* **1995**, 2031. (e) Park, S.-B.; Murata, K.; Matsumoto, H.; Nishiyama, H. *Tetrahedron: Asymmetry* **1995**, *6*, 2487. (f) Schnyder, A.; Togni, A.; Wiesli, U. *Organometallics* **1997**, *16*, 255. (g) Palucki, M.; Finney, N. S.; Pospisil, P. J.; Güler, M. L.; Ishida, T.; Jacobsen, E. N. *J. Am. Chem. Soc.* **1998**, *120*, 948.

10.1021/om980980k CCC: $18.00
Publication on Web 03/05/1999

eters arguably influence the properties of a catalytically active metal center simultaneously.[6]

The chemical shift of a transition metal is a very sensitive probe for electronic *and* geometric changes in the coordination sphere of the nucleus under scrutiny.[7−10] Although there is no a priori reason for an intrinsic relation between NMR shifts and chemical reactivity, a number of empirical correlations of this type have been established.[9b−e,11−13] In a seminal study, Bönnemann and von Philipsborn correlated ^{59}Co shifts and catalytic properties of substituted cyclopentadienyl Co(I) complexes.[12] Similarly, direct relationships between ^{103}Rh shifts and rate constants have been described for stoichiometric exchange processes involving cyclopentadienyl Rh(I)[9b] and Rh(III)[9c] complexes. The chemical shift difference between the diastereomeric intermediates in catalytic hydrogenation of prochiral olefins using chiral phosphine rhodium complexes has been related to the enantioselective discrimination.[9d] More recently, Åkermark et al. have correlated stability constants of complexes [(acac)Rh(alkene)$_2$] with ^{103}Rh shifts.[9e]

We have recently introduced the four-coordinate 16e complexes [(P$_2$)Rh(hfacac)] (hfacac = hexafluoroacetylacetonate) as model compounds for the investigation of the intrinsic influence of bidentate chelating ligands on structure, reactivity, and spectroscopic properties of the [(P$_2$)Rh] fragment.[13] Experimental data for structurally closely related compounds suggested a potentially useful empirical correlation between the ^{103}Rh shifts of complexes [(P$_2$)Rh(hfacac)] and their catalytic activity in the hydrogenation of CO_2 to formic acid.[13a] During extension of these studies to a broader range of ligands, however, the connections between structural features, ^{103}Rh shifts, and chemical reactivity were found to be very subtle.[13b]

To proceed from purely empirical correlations in practical systems to a deeper understanding of the underlying principles, the intrinsic influence of the controlling ligand on the NMR shift of the metal center in the [(P$_2$)Rh] fragment has to be elucidated. Despite an increasing body of data,[10,13] in particular from the seminal work by the group of Elsevier,[10a,b] the factors governing ^{103}Rh shifts in Rh(I) phosphine complexes are far from being fully understood. A detailed analysis of the solid state NMR data of related complexes containing [(P$_2$)M] (M = Mo, W, Pt) fragments by Lindner et al. has revealed a remarkable sensitivity of the principal components of the ^{31}P chemical shift tensor on small structural changes, suggesting that changes in the coordination geometry might play a major role in determining the chemical shift of the corresponding metal centers as well.[14] Recently, density-functional theory based calculations have been shown to reliably reproduce trends in $\delta(^{103}Rh)$ shifts for various rhodium complexes[15] and may thus help in the interpretation of experimental results obtained from systematic studies.

Herein we present a detailed experimental and computational study on the influence of the geometrical and electronic properties of chelating phosphine ligands on the ^{103}Rh chemical shift in complexes containing [(P$_2$)Rh] fragments. For neutral 1,3-diketonato complexes, electronic variation was achieved by introducing substituents with different inductive effects in the *para* position of a chelating bis(aryl)phosphine. Geometric parameters, for instance P−Rh−P angles ranging from 70° to 100°, were adjusted by variations in the backbone and the groups R at phosphorus. In addition, selected ionic complexes containing the [(P$_2$)Rh] fragment were investigated for comparison.

Experimental Section

General Remarks. All reactions involving air- or moisture-sensitive materials were performed under argon using standard Schlenk techniques in dried and deoxygenated solvents. The complexes [(cod)Rh(hfacac)] (cod = 1,5-cyclooctadiene, **4**)[16] and [(P$_2$)Rh(hfacac)][13b] (**7**, **9b**−**d**, **11**) were synthesized as described previously. The ligands **6**, **8**, **10** were commercial products or prepared following known procedures.[17] $Cl_2P(CH_2)_4$-

(6) For interesting investigations on the relationship between bite angle and electronic structure see: Hofmann, P.; Meier, C.; Englert, U.; Schmidt, M. U. *Chem. Ber.* **1992**, *125*, 353.

(7) (a) Benn, R.; Rufińska, A. *Angew. Chem.* **1986**, *98*, 851; *Angew. Chem., Int. Ed. Engl.* **1986**, *25*, 861. (b) von Philipsborn, W. *Pure Appl. Chem.* **1986**, *58*, 513. (c) Mason, J. *Chem. Rev.* **1987**, *87*, 1299. (d) Pregosin, P. S., Ed. *Transition Metal Nuclear Magnetic Resonance*; Elsevier: Amsterdam, 1991. (e) von Philipsborn, W. *Chem. Soc. Rev.*, in press.

(8) For recent examples with transition metals other than rhodium: *^{55}Mn*: Dowler, M. E.; Le, T. X.; DeShong, P.; von Philipsborn, W.; Vöhler, M.; Rentsch, D. *Tetrahedron* **1993**, *49*, 5673. *^{187}Os*: Bell, A. G.; Koźmiński, W.; Linden, A.; von Philipsborn, W. *Organometallics* **1996**, *15*, 3124. *^{91}Zr*: Bühl, M.; Hopp, G.; Beck, S.; Prosenc, M.-H.; Rief, U.; Brintzinger, H.-H. *Organometallics* **1996**, *15*, 778. *^{57}Fe*: Benn, R.; Brenneke, H.; Frings, A.; Lehmkuhl, H.; Mehler, G.; Rufińska, A.; Wildt, T. *J. Am. Chem. Soc.* **1988**, *110*, 5561. Meier, E. J. M.; Koźmiński, W.; Linden, A.; Lustenberger, P.; von Philipsborn, W. *Organometallics* **1996**, *15*, 2469.

(9) For recent examples with rhodium and variation in ligands other than phosphines: (a) Graham, P. B.; Rausch, M. D.; Täschler, K.; von Philipsborn, W. *Organometallics* **1991**, *10*, 3049. (b) Koller, M.; von Philipsborn, W. *Organometallics* **1992**, *11*, 467. (c) Tedesco, V.; von Philipsborn, W. *Organometallics* **1995**, *14*, 3600. (d) Bender, B. R.; Koller, M.; Nanz, D.; von Philipsborn, W. *J. Am. Chem. Soc.* **1993**, *115*, 5889. (e) Åkermark, B.; Blomberg, M. R. A.; Glaser, J.; Öhrström, L.; Wahlberg, S.; Wärnmark, K.; Zetterberg, K. *J. Am. Chem. Soc.* **1994**, *116*, 3405. (f) Brunet, J.-J.; Commenges, G.; Neibecker, D.; Philippot, K.; Rosenberg, L. *Inorg. Chem.* **1994**, *33*, 6373. (g) Law, D. J.; Bigam, G.; Cavell, R. G. *Can. J. Chem.* **1995**, *73*, 635. (h) Asaro, F.; Costa, G.; Dreos, R.; Pellizer, G.; von Philipsborn, W. *J. Organomet. Chem.* **1996**, *513*, 193. (i) Donkervoort, J. G.; Bühl, M.; Ernsting, J. M.; Elsevier, C. J. *Eur. J. Inorg. Chem.* **1999**, 27.

(10) For recent examples of rhodium complexes with structural variations in phosphorus ligands: (a) Ernsting, J. M.; Elsevier, C. J.; de Lange, W. G. J.; Timmer, K. *Magn. Reson. Chem.* **1991**, *29*, S118. (b) Elsevier, C. J.; Kowall, B.; Kragten, H. *Inorg. Chem.* **1995**, *34*, 4836. (c) Carlton, L. *J. Organomet. Chem.* **1992**, *43*, 103. (d) Cherkasova, T. G.; Varshavsky, Yu. S.; Podkorytov, I. S.; Osetrova, L. V. *Rhodium Express* **1993**, *0*, 21. (e) Gavrilov, K. N.; Ignatenko, A. V.; Teleshev, A. T. *Russ. J. Coord. Chem.* **1995**, *21*, 461. (f) Börner, A.; Kless, A.; Holz, J.; Baumann, W.; Tillack, A.; Kadyrov, R. *J. Organomet. Chem.* **1995**, *490*, 213. (g) Börner, A.; Kless, A.; Kempe, R.; Heller, D.; Holz, J.; Baumann, W. *Chem. Ber.* **1995**, *128*, 767. (h) Jolly, P. W.; Hopp, G.; Passelaigne, E.; von Philipsborn, W. Personal communications.

(11) For a computational prediction of such a correlation for vanadium-catalyzed ethylene polymerization see: Bühl, M. *Angew. Chem., Int. Ed. Engl.* **1998**, *37*, 142.

(12) (a) Bönnemann, H.; Brijoux, W.; Brinkmann, R.; Meurers, W.; Mynott, R.; von Philippsborn, W.; Egolf, T. *J. Organomet. Chem.* **1984**, *272*, 231. (b) Bönnemann, H. *Angew. Chem.* **1985**, *97*, 264; *Angew. Chem., Int. Ed. Engl.* **1985**, *24*, 248. (c) For other examples for relations between structure and ^{59}Co shifts see: Benn, R.; Cibura, K.; Hoffmann, P.; Jonas, K.; Rufińska, A. *Organometallics* **1985**, *4*, 2214.

(13) (a) Fornika, R.; Görls, H.; Seemann, B.; Leitner, W. *J. Chem. Soc., Chem. Commun.* **1995**, 1479. (b) Angermund, K.; Baumann, W.; Dinjus, E.; Fornika, R.; Görls, H.; Kessler, M.; Krüger, C.; Leitner, W.; Lutz, F. *Chem. Eur. J.* **1997**, *3*, 755.

(14) Lindner, E.; Fawzi, R.; Mayer, H. A.; Eichele, K.; Hiller, W. *Organometallics* **1992**, *11*, 1033.

(15) (a) Bühl, M. *Organometallics* **1997**, *16*, 261. (b) Bühl, M. *Chem. Phys. Lett.* **1997**, *267*, 251.

(16) Leipoldt, J. G.; Grobler, E. C. *Trans. Met. Chem.* **1986**, *11*, 110.

(17) (a) Issleib, K.; Müller, D.-W. *Chem. Ber.* **1959**, *92*, 1397. (b) Burt, R. J.; Chatt, J.; Hussein, W.; Leigh, G. J. *J. Organomet. Chem.* **1979**, *182*, 203. (c) Brunner, H.; Lautenschlager, H.-J. *Synthesis* **1989**, 706. (d) Dinjus, E.; Leitner, W. *Appl. Organomet. Chem.* **1995**, *9*, 43.

PCl_2 (**1**) was synthesized according to the method of Kuchen.[18]

Mass spectra were measured on a Finnigan MAT SSQ 710 with EI-MS technique. Standard NMR spectra were recorded in 5 mm tubes on a Bruker AC 200 spectrometer operating at 200.13, 50.29, 188.15, and 80.15 MHz for ^{1}H, ^{13}C, ^{19}F, and ^{31}P. Chemical shifts δ are reported in ppm relative to external $CFCl_3$ for ^{19}F, H_3PO_4 for ^{31}P, and TMS for ^{1}H and ^{13}C, using the solvent resonance as a secondary standard if possible. Coupling constants J are given in hertz.

Solid State NMR. Solid state CP/MAS NMR spectra were recorded as described previously[19] on a Bruker MSL-300 spectrometer operating at 121.5 MHz for ^{31}P and 75.47 MHz for ^{13}C using NaH_2PO_4 (δ 0.314 relative to 85% H_3PO_4) and adamantane (δ 38.40 relative to TMS) as an external standard, respectively. Coupling constants J(PP′) were determined from J resolved 2D spectra.[19,20]

Determination of δ(^{103}Rh). 2D(^{31}P,^{103}Rh{^{1}H}) spectra were recorded on a Bruker ARX 400 spectrometer (B_0 = 9.4 T) at 298 K. The standard four-pulse HMQC sequence[21] was performed twice with variation of the ^{103}Rh frequency offset and the t_1 increment to ensure that signals in the F_1 dimension (^{103}Rh) are not folded. Typical conditions: 128 experiments in t1, 4 or 8 scans each, 4 s relaxation delay, total experimental time ca. 40−80 min. The ^{103}Rh shifts are given relative to $\Xi(^{103}Rh) = 3.16$ MHz[7,22] and were reproducible within 1 ppm.

Synthesis of Phosphine Ligands 3a−e. A solution of $Cl_2P(CH_2)_4PCl_2$ (1.14 mL, 6.00 mmol) in 10 mL of THF was added dropwise to a THF solution containing 23.9 mmol of p-XC_6H_4MgBr at −30 °C. The resulting mixture was allowed to warm to room temperature and stirred for 1 h. Dioxane (20 mL) was added, and the solution was filtered over Celites. The filtrate was washed with 20 mL of aqueous NH_4Cl solution, and the aqueous phase was extracted with THF (2 × 10 mL). The combined organic layers were dried over $MgSO_4$ and filtered, and the solvents were removed in vacuo. The resulting off-white or slightly yellow products were recrystallized from EtOH to give the colorless ligands (40−80% yield) in >95% purity (^{1}H, ^{31}P NMR). Selected spectroscopic data are summarized in Table 1; full details are available as Supporting Information.

Synthesis of Complexes 5a−e. One equivalent of the appropriate chelating phosphine **3a**−**e** in 15 mL of THF was added dropwise to a solution of **4** (300 mg, 0.72 mmol) in 15 mL of THF at −78 °C. The reaction mixture was allowed to warm to room temperature, and the volatiles were removed in vacuo. The glassy residues were dried under vacuum for 24 h to yield quantitatively **5a**−**e** as red-brown powders containing small amounts of THF and cyclooctadiene, but less than 5% phosphorus-containing impurities according to NMR analyses. The ^{103}Rh chemical shifts were determined from these samples without further purification. Characteristic spectroscopic data are given in Table 1; full details including MS and ^{13}C NMR data are available as Supporting Information.

Synthesis and X-Ray Crystal Structure Analysis of Complex 9a. The procedure was essentially the same as described earlier for **9b**,[13b] using solutions of **4** (414 mg, 0.99 mmol) and **8a** (405 mg, 0.99 mmol) in 40 mL of THF each. Addition of the phosphine solution was carried out extremely slowly in order to avoid formation of the doubly substituted complex [(**8a**)$_2$Rh][hfacac][13b] and/or bridged binuclear complexes (see text for details). Crystallization of the crude product from ^{t}BuOMe afforded analytically pure **9a** as deeply red, almost black crystals suitable for X-ray diffraction.

9a: 582 mg (0.81 mmol, 82%), mp 115 °C. Anal. ($C_{30}H_{47}F_6O_2P_2Rh$) C; H; F; P: calcd, 50.15, 6.59, 15.86, 8.62; found, 50.08, 6.58, 16.08, 8.59. MS (EI): m/z 718 ($M^{\bullet+}$, 100), 636 ($M^{\bullet+} - C_6H_{10}$, 31), 545 ($M^{\bullet+} - 2C_6H_{10}$, 23).

IR (KBr): 2925 s (ν(CH_2), Cy), 2852 s (ν(CH_2), Cy), 2665 w, 2654 w, 1672 w, 1621 w, 1593 m (ν(C═O) hfacac), 1565 m, 1536 m, 1504 m, 1479 m (ν(C═O) hfacac), 1447 m (δ(CH_2)), 1335 m, 1254 s (CF_3), 1193 s, 1143 s (CF_3), 1095 m, 1076 m, 1068 m, 1024 w, 1000 m, 942 m, 914 w, 888 m, 851 m, 812 w, 784 m, 759 m, 741 w, 721 m, 677 m, 588 m, 531 m, 510 m cm^{-1}.

^{1}H NMR (THF-d_8): δ 5.95 (1H, s, C*H*(CF_3)), 2.50 (2H, dt, ^2J(PH) = 9 Hz, ^3J(RhH) = 3 Hz, CH_2(PCy_2)$_2$) 2.12−1.14 (44H, m, Cy-*H*) ppm. ^{13}C{^{1}H} NMR (THF-d_8): δ 171.0 (q, ^2J(FC) = 33.0 Hz, *C*O), 120.1 (q, ^1J(FC) = 284 Hz, *C*F_3), 90.1 (s, *C*HC(CF_3)), 27.7 (dt, ^1J(PC) = 9.5 Hz, ^2J(RhC) = 6.5 Hz, CH_2(PCy_2)$_2$) 37.0(m)/30.4(s)/30.3(s)/27.94(m)/27.90(m)/27.1(s) (Cy−*C*) ppm. ^{19}F{^{1}H} NMR (THF-d_8): δ −76.7 ppm. ^{31}P{^{1}H} NMR (THF-d_8): δ −4.2 (d, ^1J(RhP) = 164 Hz) ppm. 2D(^{31}P,^{103}Rh) {^{1}H} NMR (THF-d_8): δ 1062 ppm. ^{13}C{^{1}H} CP/MAS NMR (297 K): δ 170.2/169.6 (*C*O), 119.9 (q, ^1J(FC) = 290 Hz, *C*F_3), 89.8 (s, *C*HC(CF_3)), 43.1 − 27.2 (*C*H_2(PCy_2)$_2$, Cy−*C*). ^{31}P{^{1}H} CP/MAS NMR (310 K): δ −5.6 (dd, ^2J(PP′) = 117 ± 5 Hz, ^1J(RhP) = 164 ± 5 Hz, P), −6.7 (dd, ^2J(P′P) = 117 ± 5 Hz, ^1J(RhP′) = 170 ± 5 Hz, P′).

Crystal Data of 9a: $C_{30}H_{47}F_6O_2P_2Rh$, M = 718.53, trigonal, space group $R\bar{3}c$ (No. 167), $a = b = c$ = 17.6900(9) Å, $\alpha = \beta = \gamma$ = 96.738(4)°, V = 5411.2(5) Å^3 (λ = 0.710 69 Å), Z = 6, ρ_c = 1.323 g cm^{-3}, F(000) = 2232. Crystal dimensions 0.32 × 0.46 × 0.46 mm^3, μ = 6.16 cm^{-1}.

Data Collection and Processing. Data were collected on an Enraf-Nonius CAD4 diffractometer in the $\omega/2\theta$ scan mode using graphite-monochromated Mo Kα radiation. Unit cell parameters were determined from least-squares refinement of setting angles for 25 reflections. Data were corrected for Lorentz and polarization effects. There was no correction for crystal decay. A total of 5368 (904 independent) reflections were measured ($1.76 \le \theta \le 27.45$, $1 \le h \le 22$, $0 \le k \le 15$, $0 \le l \le 11$) at T = 293(1) K.

Structure Analysis and Refinement. The structure was solved by the heavy atom method using SHELX-93.[23] Refinement was by full-matrix least-squares on F^2 with 413 positional and anisotropic thermal parameters for non-H atoms. H atoms were fixed at calculated positions with C−H = 0.96 Å and an overall temperature factor. No absorption correction was applied. Weighting scheme $w = q/[\sigma^2(F_o^2) + (0.0641P)^2 + 12.2717P]$ where $P = (F_o^2 + 2F_c^2)/3$. Final R indices ($I > 2\sigma(I)$), R = 0.0653 and wR^2 = 0.2068; residual electron density 0.478 e Å^{-3}. Essential geometric molecular data are depicted in Figure 2.

Synthesis of Complex 9c. Complex **9c** was obtained as brown powder according to the method described for **5a**−**e**, using solutions of **4** (265 mg, 0.63 mmol) and **8c** (278 mg, 0.64 mmol) in 20 mL of THF each. Crystallization from ^{t}BuOMe gave 425 mg (0.57 mmol, 90%) of **9c** in the form of a brown microcrystalline powder.

^{1}H NMR (THF-d_8): δ 6.02 (1H, s, C*H*(CF_3)), 2.30 (2H, d, ^2J(PH) = 12 Hz, CH_2(PCy_2)$_2$) 1.95−1.10 (46H, m, Cy-*H*) ppm. ^{13}C{^{1}H} NMR (THF-d_8): δ 170.9 (q, ^2J(FC) = 33.4 Hz, *C*O), 120.2 (q, ^1J(FC) = 285 Hz, *C*F_3), 90.0 (s, *C*HC(CF_3)), 19.2 (dt, $|^1J(PC) + {}^3J(P'C)|$ = 32.4 Hz, ^2J(RhC) = 1.9 Hz, CH_2(PCy_2)$_2$), 24.1 (d, ^2J(RhC) = 2.9 Hz, CH_2CH_2(PCy_2)$_2$) 36.9(m)/30.9(s)/29.9(s)/28.4(m)/28.2(m)/27.4(s) (Cy−*C*) ppm. ^{19}F{^{1}H} NMR (THF-d_8): δ −76.8 ppm. ^{31}P{^{1}H} NMR (THF-d_8): δ 42.7 (d, ^1J(RhP) = 186 Hz) ppm. 2D(^{31}P,^{103}Rh) {^{1}H} NMR (THF-d_8): δ 608 ppm.

(18) Diemert, K.; Kuchen, W.; Kutter, J. *Phosphorus Sulfur* **1983**, *15*, 155.
(19) Bach, I.; Pöschke, K.-R.; Goddard, R.; Kopiske, C.; Krüger, C.; Rufińska, A.; Seevogel, K. *Organometallics* **1996**, *15*, 4959.
(20) Wu, G.; Wasylishen, R. E. *Inorg. Chem.* **1992**, *31*, 145.
(21) Bax, A.; Griffey, R. H.; Hawkins, B. L. *J. Magn. Reson.* **1983**, *55*, 301.
(22) Mann, B. E. In *Transition Metal Nuclear Magnetic Resonance*; Pregosin, P. S., Ed.; Elsevier: Amsterdam, 1991; p 177.
(23) Sheldrick, G. M. *SHELXL-93*, Program for Crystal Structure Refinement; University Göttingen: Germany, 1993.

Scheme 1. Synthesis of *para*-Substituted Ligands $Ar_2P(CH_2)_4PAr_2$ Forming Seven-Membered Chelate Rings upon Coordination

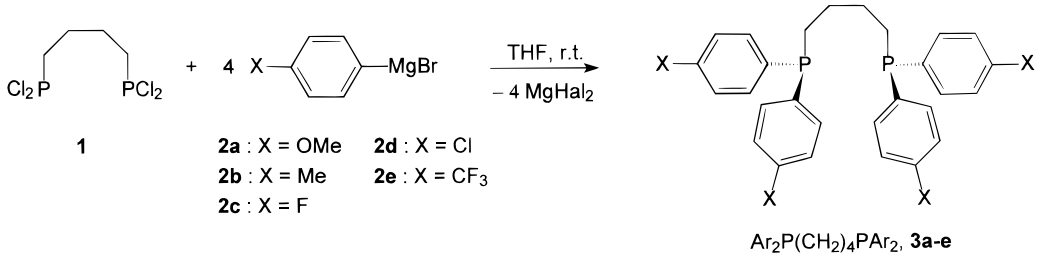

1

2a : X = OMe **2d** : X = Cl
2b : X = Me **2e** : X = CF_3
2c : X = F

$Ar_2P(CH_2)_4PAr_2$, **3a-e**

Scheme 2. Synthesis of Neutral Complexes [{$R_2P(CH_2)_nPR_2$}Rh(hfacac)]

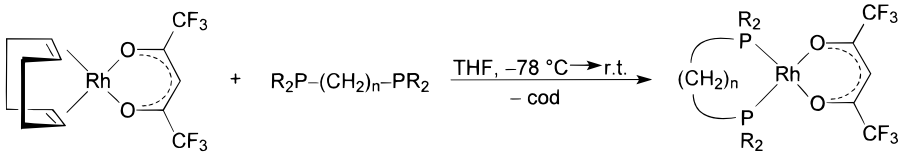

4

3a-e: R = Ar, n = 4
6a-d: R = Ph, n = 1-4
8a-d: R = Cy, n = 1-4
10: R = Me, n = 2

5a-e
7a-d
9a-d
11

Computational Details. Geometries have been fully optimized with the Gaussian 94 package[24] employing the gradient-corrected density functionals of Becke (1988)[25] and Perdew (1986)[26] for exchange and correlation, respectively, together with a quasi-relativistic effective core potential and the corresponding [6s5p3d] valence basis set for Rh,[27] and standard 6-31G* basis[28] on the ligands (designated BP86/ECP1).

Magnetic shielding tensors have been computed with the GIAO (gauge-including atomic orbitals−DFT method as implemented[29] in the Gaussian 94 program, employing Becke's three-parameter exchange DFT/Hartree−Fock hybrid functional[30] and the correlation functional of Lee, Yang, and Parr,[31] a fine integration grid (finegrid option), together with basis II, i.e., a well-tempered [16s10p9d] basis[32] on Rh (contracted from the 22s14p12d set and augmented with two d-shells of the well-tempered series) and the recommended IGLO-basis II[33] for the ligands (which is essentially of polarized triple-ζ quality), designated GIAO-B3LYP/II. Experimental ^{103}Rh chemical shifts of a number of rhodium complexes have been well reproduced using this particular combination of theoretical methods.[15b] Theoretical relative ^{103}Rh chemical shifts (referenced to the usual standard frequency of $\Xi = 3.16$ MHz) have been calculated as $\delta = \sigma$(standard) $- \sigma$(calc), employing the σ(standard) value from ref 15b, −878 ppm. This value has been obtained from σ(calc) vs δ(expt) linear regressions employing BP86/ECP1 geometries.

Topological analysis of the total electron density has been performed using the MORPHY program[34] and the B3LYP/II′ density, i.e., employing basis II only on Rh, on the P atoms, and on the 1,3-propanedionato moiety, and IGLO-basis DZ[33] on the rest of the ligands.

Results and Discussion

1. Neutral Complexes of the Type [(P_2)Rh(1,3-diketonate)]. Investigation of Electronic Effects. Chelating phosphines **3a**−**e** were synthesized bearing electron-withdrawing or -donating substituents in the *para* position of the phenyl rings of the well-known dppb ligand **6d**, in order to probe the influence of electronic properties of the phosphine ligand on the ^{103}Rh shift. It is well established that *para* substituents in aryl phosphorous compounds do not affect the steric properties of a given ligand.[2a,b] The phosphines **3a**−**e** were obtained in reasonable to good yields by reaction of bis(dichlorophosphino)butane[18] **1** with the appropriate aryl Grignard reagents **2a**−**e** according to Scheme 1. The neutral Rh(I) complexes [(**3a**−**e**)Rh(hfacac)] (**5a**−**e**) were isolated as dark red-brown glassy solids from the reaction of [(cod)Rh(hfacac)] (**4**) with 1 equiv of **3a**−**e** in THF in analogy with the synthesis of the unsubstituted parent complex **7d** (Scheme 2).[13b] Selected spectroscopic data of the free ligands **3a**−**e**, **6d** and the complexes **5a**−**e**, **7d** are summarized in Table 1 together with the Hammett σ_p constants[35] for the substituents X.

The variations in the ^{13}C chemical shifts of the *ipso*-carbon atoms in **3a**−**e**, **6d** and **5a**−**e**, **7d** upon substitution are noticeable, whereas changes in $\delta(^{31}P)$ are relatively small. In both cases, no direct relationship between Hammett σ_p constants and chemical shifts are revealed. In contrast, $\delta(^{103}Rh)$ of **5a**−**e**, **7d** can be directly correlated with σ_p, but variations are also

(24) Frisch, M. J.; Trucks, G. W.; Schlegel, H. B.; Gill, P. M. W.; Johnson, B. G.; Robb, M. A.; Cheeseman, J. R.; Keith, T.; Petersson, G. A.; Montgomery, J. A.; Raghavachari, K.; Al-Laham, M. A.; Zakrzewski, V. G.; Ortiz, J. V.; Foresman, J. B.; Peng, C. Y.; Ayala, P. Y.; Chen, W.; Wong, M. W.; Andres, J. L.; Replogle, E. S.; Gomperts, R.; Martin, R. L.; Fox, D. J.; Binkley, J. S.; DeFrees, D. J.; Baker, J.; Stewart, J. J. P.; Head-Gordon, M.; Gonzales, C.; Pople, J. A. *Gaussian 94*; Pittsburgh, PA, 1995.
(25) Becke, A. D. *Phys. Rev. A* **1988**, *38*, 3098.
(26) Perdew, J. P. *Phys. Rev. B* **1986**, *33*, 8822; **1986**, *34*, 7406.
(27) Andrae, D.; Häussermann, U.; Dolg, M.; Stoll, H.; Preuss, H. *Theor. Chim. Acta* **1990**, *77*, 123.
(28) Hehre, W. J.; Radom, L.; Schleyer, P. v. R.; Pople, J. A. *Ab Initio Molecular Orbital Theory*; Wiley: New York, 1986.
(29) Cheeseman, J. R.; Trucks, G. W.; Keith, T. A.; Frisch, M. J. *J. Chem. Phys.* **1996**, *104*, 5497.
(30) Becke, A. D. *J. Chem. Phys.* **1993**, *98*, 5648.
(31) Lee, C.; Yang, W.; Parr, R. G. *Phys. Rev. B* **1988**, *37*, 785.
(32) Huzinaga, S.; Klobukowski, M. *J. Mol. Struct.* **1988**, *167*, 1.
(33) Kutzelnigg, W.; Fleischer, U.; Schindler, M. In *NMR Basic Principles and Progress Vol. 23*; Springer Verlag: Berlin, 1990; p 165.
(34) Popelier, P. L. A. *Comput. Phys. Commun.* **1996**, *93*, 212.
(35) Note that Hammett constants and absolute magnetic shieldings have the same notations and should not be confused. The values for σ_p used here are taken from: March, J. *Advanced Organic Chemistry*, 3rd ed.; Wiley: New York, 1985; p 244.

Table 1. Selected Analytical Data of Free Ligands $(p\text{-}XC_6H_4)_2P(CH_2)_4P(p\text{-}XC_6H_4)_2$[a] 6d, 3a−e and Corresponding Complexes [(P_2)Rh(hfacac)] 7d, 5a−e [b]

	X	δ (^{13}C)[c] (ligand) [ppm]	δ (^{13}C)[c] (complex) [ppm]	δ (^{13}P) (ligand) [ppm]	δ (^{13}P) (complex) [ppm]	J_{RhP} (complex) [ppm]	δ (^{103}Rh) (complex) [ppm]	σ_P[e] (Hammett)
6d/7d	H	138.7	137.3	−14.3[d]	48.6	191	623	0
3a/5a	OMe	129.9	128.6	−19.1	45.5	192	646	−0.28
3b/5b	Me	135.4	134.3	−17.5	46.8	191	639	−0.14
3c/5c	F	134.2	132.8	−18.0	47.8	191	599	0.15
3d/5d	Cl	136.8	136.6	−17.3	48.4	191	589	0.24
3e/5e	CF_3	143.1	141.2	−14.2	50.3	190	570	0.53

[a] In $CDCl_3$. [b] In THF-d_8. [c] Aromatic ipso-carbon directly bound to phosphorus. [d] In benzene-d_6. [e] See ref 35.

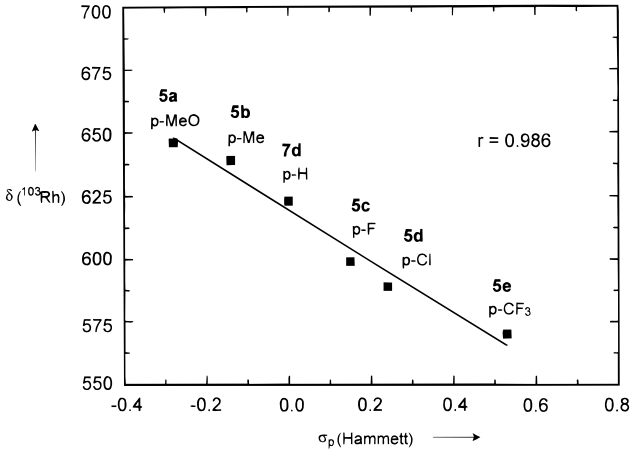

Figure 1. Correlation between $\delta(^{103}Rh)$ and Hammett σ_P constants[35] for complexes [{$(p\text{-}XC_6H_4)_2P(CH_2)_4P(p\text{-}XC_6H_4)_2$}-Rh(hfacac)] (**5a**−**e**, **7d**).

moderate, within less than 80 ppm (Figure 1). Correlations with the Hammett σ_P constants have been established also for the basicity of related aryl phosphines[36] and are generally interpreted in terms of inductive effects. Thus, the same inductive effects will affect the HOMO−LUMO gap and lead to variations in the paramagnetic contribution of the magnetic shielding. Apparently, such inductive effects have very little impact on the ^{103}Rh chemical shift in complexes containing the [(P_2)Rh] fragment.[10a,b]

Investigation of Geometrical Effects. Coordination geometries of complexes [{$R_2P(CH_2)_nPR_2$}Rh(hfacac)] can be controlled by the length *n* of the chelate backbone and the steric bulk of the substituents R.[13] The size of the P−Rh−P angle together with the bulkiness of the groups R and the flexibility of the chelate ring can play an important role for the behavior of the [(P_2)Rh] fragment in catalytic reactions, as has recently been rationalized in the so-called accessible molecular surface (AMS) model.[13b] In the series of compounds **7b**−**d** and **9b**−**d** with $n = 2-4$, larger chelate rings were shown to be associated with a deshielding of the ^{103}Rh nucleus and with an enhanced catalytic activity for CO_2 hydrogenation, independent of the substituent R. At the same time, the P−Rh−P angle as determined by X-ray crystallographic analyses showed an apparent linear correlation with $\delta(^{103}Rh)$.[13]

Introduction of the methylene-bridged ligands $R_2PCH_2PR_2$ (R = Ph, **6a**; R = Cy, **8a**) using the same methodology as for $n \geq 2$ affords complexes **7a** and **9a**, which are, however, characterized by strongly deshielded ^{103}Rh nuclei with $\delta(^{103}Rh) = 1130$ and 1062, respectively. The experimentally determined ^{103}Rh chemical shifts for the systematic series of neutral complexes [{$R_2P(CH_2)_nPR_2$}Rh(hfacac)] with R = Ph (**7a**−**d**) and R = Cy (**9a**−**d**) are compiled in Table 2. Independent of the substituent at phosphorus, the dependence of $\delta(^{103}Rh)$ on the length *n* of the chelate bridge shows the typical U-shaped behavior for $1 \leq n \leq 4$: With respect to the five-membered chelate rings **7b** and **9b**, both smaller and larger rings in the respective series are characterized by strong deshielding of the ^{103}Rh chemical shift.[10a,b,14] However, an increased shielding rather than a deshielding of the ^{103}Rh nuclei would be anticipated for the small P−Rh−P angles in **7a**, **9a** if the above described empirical correlation for $n \geq 2$ would be generally valid.

Table 2. Experimental and Calculated ^{103}Rh Chemical Shifts (δ in ppm) for Selected Complexes [{$R_2P(CH_2)_nPR_2$}Rh(1,3-diketonate)]

R	*n* = 1	*n* = 2	*n* = 3	*n* = 4
Ph	**7a**: 1130[a]	**7b**: 438[a]	**7c**: 567[a]	**7d**: 623[b]
Cy	**9a**: 1062[b]	**9b**: 368[a]	**9c**: 608[b]	**9d**: 845[a]
Me	**12a**: 1466[c]	**12b**: 514[c]	**12c**: 659[c]	**12d**: 724[c]
		11: 370[a]		

[a] Experimental value, from ref 13. [b] Experimental value, this work. [c] From DFT calculations on the acac model compounds **12a**−**d** without additional constraints.

Elucidation of the molecular structure of **9a** by single-crystal X-ray diffraction analysis (Figure 2) unambiguously proves that it exists as a mononuclear 16e complex bearing a four-membered chelate ring in the solid state.[37] The rhodium atom and the two central carbon atoms of the phosphine and the hfacac chelate rings reside on a C_2 symmetry axis. The CF_3 groups are in statistical disorder as observed also in other solid state structures of Rh−hfacac complexes.[13b] Bond lengths and angles within the four-membered chelate[38,39] and within the hfacac ligand[13b] are in the range expected from other Rh(I) complexes containing similar moieties. The coordination geometry about Rh is slightly distorted from an ideal square planar arrangement with an angle θ between the O−Rh−O and P−Rh−P planes of 12.6°.

(36) Bush, R. C.; Angelici, R. J. *Inorg. Chem.* **1988**, *27*, 681.

(37) The ability of bis(phosphino)methane ligands to bridge two rhodium metals is well established. See for example: (a) Sanger, A. R. *J. Chem. Soc., Chem. Commun.* **1975**, 893. (b) Sanger, A. R. *J. Chem. Soc., Dalton Trans.* **1977**, 120. (c) Shafiq, F.; Kramarz, K. W.; Eisenberg, R. *Inorg. Chim. Acta* **1993**, *213*, 111. (d) Anderson, D. J.; Kramarz, K. W.; Eisenberg, R. *Inorg. Chem.* **1996**, *35*, 2688.

(38) R = Ph: Pignolet, L. H.; Doughty, D. H.; Novicki, S. C.; Casalnuovo, A. L. *Inorg. Chem.* **1980**, *19*, 2172. Chebi, D. E.; Fanwick, P. E.; Rothwell, I. P. *Organometallics* **1990**, *9*, 2948. Ge, Y.-W.; Sharp, P. R. *Inorg. Chem.* **1991**, *30*, 1671; R = ^{t}Bu, see ref 6.

(39) Fornika, R.; Görls, H.; Leitner, W.; Six, C. Manuscript in preparation.

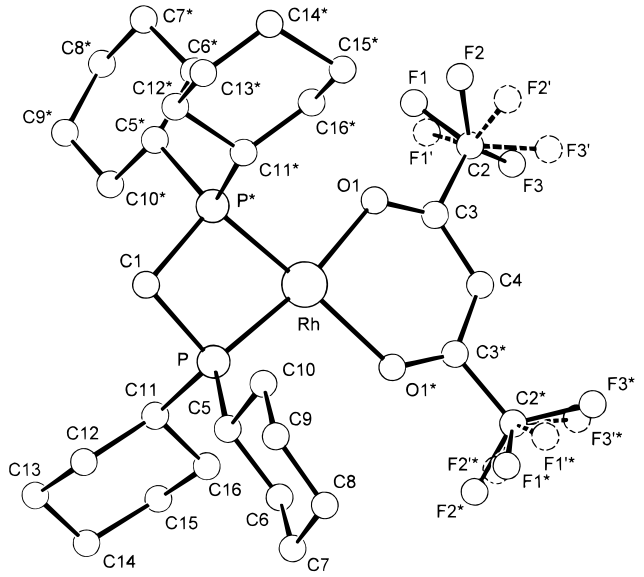

Figure 2. Molecular structure of [($Cy_2PCH_2PCy_2$)Rh(hfacac)] (**9a**) as determined by single-crystal X-ray diffraction analysis. Heavy atoms are represented as spheres, and hydrogen atoms have been omitted for clarity. Selected bond distances (Å) and angles (deg): Rh(1)−P(1), 2.195(4); P(1)−C(1), 1.840(5); P(1)−C(5), 1.79(2); P(1)−C(11), 1.90(2); Rh(1)−O(1), 2.10(1); O(1)−C(3), 1.20(2); C(3)−C(4), 1.40(2); C(2)−C(3), 1.54(3); P(1)*−Rh(1)−P(1), 73.7(2); C(1)−P(1)−Rh(1), 97.4(2); P(1)*−C(1)−P(1), 91.4(2); C(5)−P(1)−Rh(1), 124.8(7); C(11)−P(1)−Rh(1), 113.2(7); C(11)−P(1)−C(5), 107.6(9); C(5)−P(1)−C(1), 107.3(6); C(11)−P(1)−C(1), 104.0(7); O(1)*−Rh(1)−P(1); 100.0(4); O(1)−Rh(1)−P(1), 169.4(4); O(1)*−Rh(1)−O(1), 87.5(5); C(3)−O(1)−Rh(1), 125.(1); C(4)−C(3)−O(1), 129(2); C(3)*−C(4)−C(3), 123(1); C(2)−C(3)−O(1), 115(2).

In the ^{31}P CP/MAS spectra of **9a**, the isolated ^{31}P−^{31}P spin pairs of the chelating ligand are composed of two spectroscopically inequivalent nuclei with chemical shifts of −5.6 and −6.7 ppm, respectively.[14,40] A coupling constant J(P,P) = 117 ± 5 Hz was determined for **9a** by 2D-J-resolved experiments, similar to the large couplings detected in Ni(0) complexes bearing four-membered chelates of the related ligand ^{t}Bu$_2$PCH$_2$-P^{t}Bu$_2$.[41] Two distinct resonances at 170.2 and 169.6 ppm are also observed for the quaternary carbonyl carbons of the hfacac ligand in the ^{13}C CP/MAS spectra of **9a**. Allowing for the nonidentical orientations of chemical shift tensors in the solid state,[40] the similarity of the NMR data in the solid state and in solution clearly indicates that the mononuclear structure of **9a** with the four-membered chelate is retained in solution. Additional evidence is provided by the ring contribution to the ^{31}P chemical shift $\Delta\delta_R$ = 64 ppm, which is in the typical range for strained four-membered [(P_2)Rh] fragments.[42]

In addition to **9a** a minor byproduct was sometimes observed in the NMR spectra of the crude product both in solution and in the solid state. This compound was formed in variable amounts (ca. 10%) depending on the rate of addition and the reaction temperature. The values of the ^{31}P chemical shift (δ −7.2, THF-d_8; δ −9.8/−10.9, solid state) and the ^{103}Rh,^{31}P coupling constant (J(Rh,P) = 170 Hz) are very similar to those of **9a**, suggesting that this species also contains a four-membered [(P_2)Rh] fragment. Therefore, we tentatively assign this species as the hfacac-bridged dimer [(**8a**)-Rh(μ-κ^2O,O′-hfacac)$_2$Rh(**8a**)], **9a′**. In agreement with the opening of the hfacac chelate, the ^{103}Rh chemical shift of **9a′**, 326 ppm, is remarkably shielded compared to its monomeric congener **9a**. A second phosphorus-containing complex was formed from **9a** in benzene-d_6 solution upon standing (ca. 8% after 78 h) and showed an apparent doublet ($\Delta\nu$ = 101 Hz) at δ(^{31}P) = 0.6. This splitting is well in the range of the higher order coupling constants $|^1J(\mathrm{RhP}) + {}^3J(\mathrm{RhP})|$ (ca. 114 Hz) reported for binuclear complexes with **6a** as a bridging ligand (apparent doublets, AA′A″A‴XX′ spin system).[37a,b] Therefore, this second minor component can reasonably be assigned as the bridged binuclear complex [(hfacac)Rh(μ-κ^2P,P′-**8a**)$_2$Rh(hfacac)], **9a″**, although the corresponding ^{103}Rh shift was not determined. In benzene-d_6, the hfacac methine protons of **9a**, **9a′**, and **9a″** resonated at 6.24, 6.03, and 6.34 ppm, respectively, and their intensities were fully consistent with the above assignments.

The above analysis proves unambiguously that the strong deshielding of the rhodium nucleus in **7a** and **9a** is indeed an intrinsic property of the four-membered [(P_2)Rh] chelate ring of these complexes and not related to possible isomerizations in solution.[37] The deshielding effect of the small bite angle is also consistent with observations made earlier using the same chelating phosphines together with other co-ligands,[10a] but no satisfactory explanation is currently available for this fact or for the relationship between coordination geometry and δ(^{103}Rh) in general. Discussion of trends in chemical shifts of transition metal compounds hitherto usually invoked the Ramsey equation, which describes the paramagnetic contribution to the chemical shift in terms of three key contributions: electron density, radial term, and mean excitation energy.[43] However, geometric variations as imposed by structural properties of chelating ligands may affect all three terms simultaneously, and quantification or even rationalization is therefore often a matter of ambiguity.[10a] Hence, we decided to adopt an alternative approach by separating the individual geometric effects on δ(^{103}Rh) using the established tools of DFT calculations for chemical shifts of transition metals.[15,44] The acetylacetonate model compounds **12a**−**d** and **13** were used in these calculations (Chart 1).

The geometries of model complexes [{$R_2P(CH_2)_nPR_2$}-Rh(acac)] (acac = acetylacetonate, R = Me, n = 1−4; **12a**−**d**) have been optimized at the BP86/ECP1 level, and the chemical shifts were calculated at the GIAO-B3LYP/II level, Table 2). For the complex with n = 2 (**12b**, C_2 symmetry), a δ(^{103}Rh) value of 514 ppm is computed. Taking into account the generally observed shift difference of 100−150 ppm between acac and hfacac complexes,[9e,22] this value is in very good accord with the experimental value, 370 ppm for [{$Me_2P(CH_2)_2$-PMe_2}Rh(hfacac)] (**11**).[13] Direct comparison of the chemi-

(40) (a) Kubo, A.; McDowell, C. A. *J. Chem. Phys.* **1990**, *92*, 7156. (b) Davies, J. A.; Dutremez, S. *Coord. Chem. Rev.* **1992**, *114*, 61.
(41) Rufińska, A.; Nickel, T.; Pörschke, K.-R. Unpublished results.
(42) Garrou, P. E. *Chem. Rev.* **1981**, *81*, 229.
(43) Ramsey, N. F. *Phys. Rev.* **1950**, *78*, 699.
(44) Malkin, V. G.; Malkina, O. L.; Casida, M. E.; Salahub, D. R. *J. Am. Chem. Soc.* **1994**, *116*, 5898.

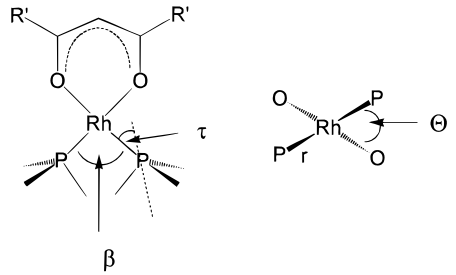

Figure 3. Definition of key geometric parameters for structural description of neutral four-coordinated complexes of the type [(P_2)Rh(1,3-diketonate)]: (left) top view; (right) projection along the pseudo-C_2 axis of the O−Rh−O chelate. See text for details.

Chart 1. Model Complexes Used for Computational Studies on Complexes [{$R_2P(CH_2)_nPR_2$}Rh(1,3-diketonate)]

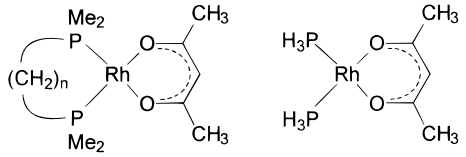

12a-d: n = 1-4 **13**

cal shifts computed for the other complexes **12a**,**c**,**d** to experimental data is difficult because of the different substituents R employed in the actual compounds. However, the aforementioned U-shaped dependence of the $\delta(^{103}Rh)$ values and their relative ordering as a function of the chelate-ring size is qualitatively reproduced by these model calculations. These results emphasize again the reliability of DFT calculations to reproduce at least qualitative trends and encouraged us to use this methodology for a detailed analysis of the relationship between coordination geometry and ^{103}Rh chemical shift.

Detailed analysis of the experimental and computed molecular structures of complexes [(P_2)Rh(1,3-diketonate)] reveals that variations in the chelate ring size are inevitably associated with changes of several geometrical parameters, notably the "bite angle" β, the P−Rh distance r, the distortion from planarity as measured by the twist angle θ, and the deviation from ideal alignment of the phosphorous lone pair with the Rh−P bond axis as measured by the "tilt angle" τ (Figure 3). These parameters cannot be varied independently in real systems,[14] as illustrated for example by a linear correlation between bite angles β and P−Rh distance r in complexes of the type [(P_2)Rh(hfacac)] (for $\beta > 82°$).[13b] To probe the individual contributions of each parameter to $\delta(^{103}Rh)$ separately, model calculations have been performed for [$(H_3P)_2$Rh(acac)] (**13**) (C_{2v} symmetry[45]). Starting from the fully optimized geometry of **13**, ^{103}Rh chemical shifts have been calculated for suitably distorted structures, i.e., by successively varying one parameter with all others fixed at constant values.

(45) Two possible orientations of the PH_3 ligands are possible for C_{2v} symmetric structures of **13**, with the hydrogen atoms in the O−Rh−P plane pointing either to the outside or to the inside of the chelate ring. Although the first one is computed to be slightly more stable, we employed the second one because of its closer resemblance to the experimental structures of the chelating bisphosphine complexes.

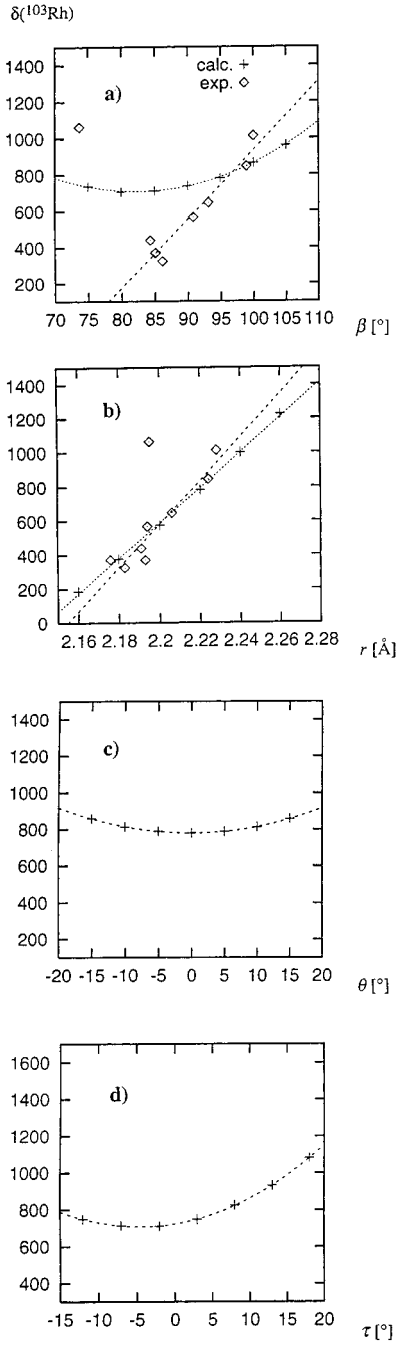

Figure 4. Variation of $\delta(^{103}Rh)$ with structural parameters (+ computed for model compound **13**, ◇ experimental data from Table 2 and ref 13); the chosen parameters (see Figure 3 for definition) and the resulting fitting functions for the theoretical data are as follows: (a) bite angle β, $\delta = 0.498(\beta - 82.4)^2 + 709$; (b) Rh−P bond length r, $\delta = 10376r - 22241$; (c) twist angle θ, $\delta = 0.344\theta^2 + 780$; (d) tilt angle τ, $\delta = 0.735(\tau + 4.5)^2 + 708$ [the form of the fitting function for τ depends somewhat on the value of β (i.e., both structural effects on δ are not simply additive); since the "increment system" of Table 4 is based on the five-membered chelate ring as standard, the β value of **12d** has been adopted during the variation of τ].

The results for the variation in β are displayed graphically in Figure 4a, together with experimental data points from the present work and ref 13. The GIAO-B3LYP data indeed show a minimum near 82°, close to the angles of 82−87° typically found[46] in five-membered P−Rh−P chelate rings. It is obvious, how-

ever, that the computed deshieldings in going to smaller or larger bite angles are far too small to account for the experimentally observed trends.

The explicit dependence of the $\delta(^{103}\text{Rh})$ values on the Rh−P bond length r computed for **13** is depicted in Figure 4b. The empirical correlation between X-ray derived Rh−P distances and experimental ^{103}Rh chemical shifts for complexes with $\beta > 82°$ noted earlier[47] is also evident from Figure 4b. With the notable exception of the four-membered chelate ring **9a** (see below), both computed (dotted line) and empirical (dashed line) correlations now appear qualitatively similar. The large slopes [10 400 ppm Å^{-1} (GIAO-B3LYP) and 12 800 ppm Å^{-1} (empirical)] indicate a large sensitivity of $\delta(^{103}\text{Rh})$ toward r. It thus appears that the ^{103}Rh chemical shifts are to a large extent governed by this bond distance, which is in turn related to the bite angle for $\beta > 82°$.[13b,47] Similar findings can be noted in the case of complexes bearing chelating amine ligands.[9i]

However, the exceptional deshielding of the ^{103}Rh nucleus in **7a**, **9a** cannot be explained solely in terms of the values of β and r; this is immediately apparent from the offset of the corresponding data points in Figure 4a,b. As noted above, the coordination geometry about the Rh atom is not planar in **9a**, with a P−Rh−P/O−Rh−O twist of $\theta = 12.6°$. Within this range of distortion, however, the twist angle θ is found to affect the computed $\delta(^{103}\text{Rh})$ value of **13** only marginally (Figure 4c).

Another geometrical feature differentiating **9a** from the other chelate complexes **9b**−**d** is the alignment of the phosphorus "lone pairs" with the respective Rh−P bond axes. Owing to the short and rigid methylene bridge in **9a**, it appears that these lone pairs are considerably tilted away from the bond axes. This less optimal alignment of the lone pairs is clearly evident in the Laplacian $\nabla^2\rho$ of the total electronic density of model compound **12a** (Figure 5a). Local charge concentrations as revealed by maxima of $-\nabla^2\rho$ reflect the shell structure of a given atom and indicate the positions of bonds and lone pairs in the valence shell.[48]

In a geometrical description, the tilt τ of the lone pair can be expressed as the angle between the direct Rh−P connection line and the pseudo-C_3 axis at the phosphorus atom, which forms identical angles to the three nearest neighbors in the phosphine moiety (Figure 3). This pseudo-C_3 axis presumably coincides with the direction of the lone pair and the proposed direction of one of the principal components of the ^{31}P shielding tensor.[14] Using this definition, the lone pairs at phosphorus are tilted by ca. 5° and 16° in the solid state structures of **9b** and **9a**, respectively. The unusually large tilt in the latter is indicative of a less efficient overlap of the orbitals involved and may thus contribute appreciably to the ^{103}Rh magnetic shielding. This notion is corroborated by ^{103}Rh chemical shift calculations for

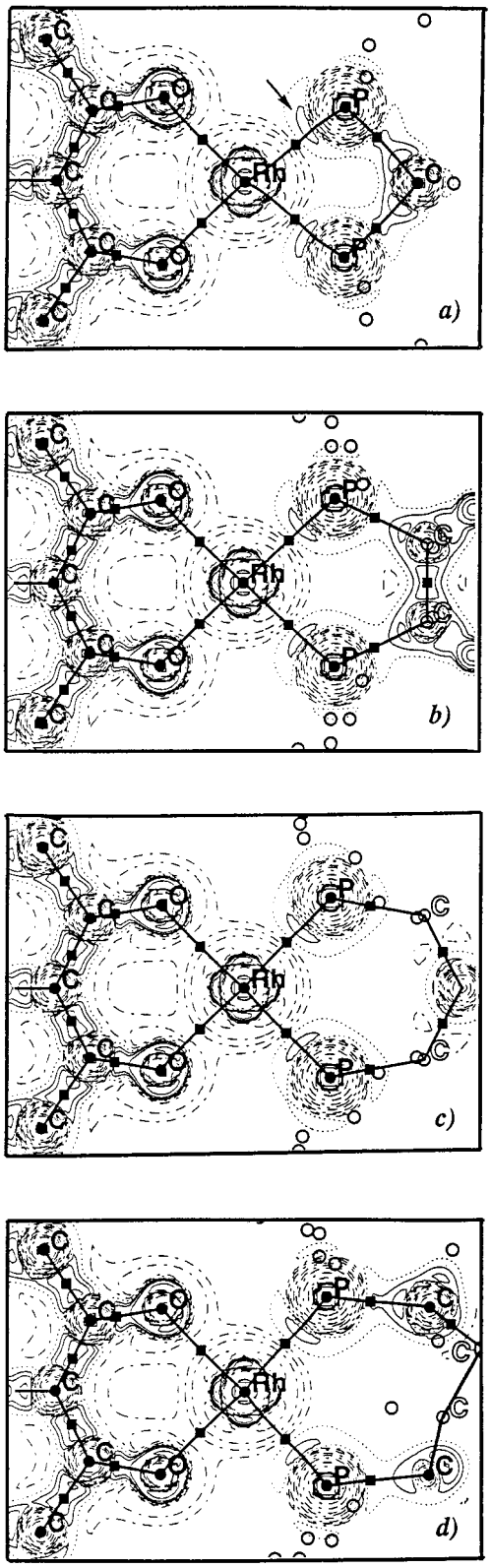

Figure 5. Negative Laplacian of the electron density, $-\nabla^2\rho$, in the P−Rh−P plane of compounds **12a**−**d** (B3LYP/II′ level). Unfilled circles and outlined labels are projections of nuclei into the plot plane. Solid lines are in regions where electronic charge is concentrated, dashed lines are in regions where charge is depleted, with contour values of $\pm 2^i \times 10^j$ atomic units ($i = 1, 2, 3$; $j = -1, 0, 1$). The arrow points to the charge concentration associated with the lone pair on a phosphorus atom of **12a**.

(46) The P−Rh−P angles of nearly all rhodium complexes with ligands $R_2P(CH_2)_2PR_2$ located in the Cambridge Structure Database are within this range.

(47) Fornika, R. Ph.D. Thesis, Friedrich-Schiller-Universität Jena, Germany, 1994.

(48) (a) Bader, R. F. W. *Atoms in Molecules. A Quantum Theory*; Clarendon Press: Oxford, 1990. (b) Bader, R. F. W. *Chem. Rev.* **1991**, *91*, 893. (c) Bader, R. F. W.; Popelier, P. L. A.; Keith, T. A. *Angew. Chem.* **1994**, *106*, 647; *Angew. Chem., Int. Ed. Engl.* **1994**, *33*, 620.

Table 3. BP86/ECP1 Optimized[a] and Experimental[b] Geometrical Parameters[c] of Selected Complexes Containing the [{$R_2P(CH_2)_nPR_2$}Rh] Fragment

	n	R	*r*	*β*	*θ*	*τ*	source
12a	1	Me	2.229	74.5	0.0	17.1	DFT
9a	1	Cy	2.195	73.7	12.6	16.1	X-ray
12b	2	Me	2.215	86.2	0.2	5.0	DFT
11	2	Me	2.176	85.1	0.0	3.7	X-ray[13]
9b	2	Cy	2.193[d]	85.0	7.6	4.2[d]	X-ray[13]
12c	3	Me	2.223	93.1	0.0	−3.0	DFT
7c	3	Ph	2.194	90.9	3.8	−3.9[d]	X-ray[13]
12d	4	Me	2.230[d]	98.8	2.0	−7.6[d]	DFT
9d	4	Cy	2.224[d]	98.9	5.1	−7.5[d]	X-ray[13]

[a] acac complexes. [b] hfacac complexes. [c] For definition, see text and Figure 3. [d] Mean value.

Table 4. Incremental ^{103}Rh Chemical Shift Changes Δδ Based on Structural Parameters Resulting from Variation of the Chain Length *n* in Complexes [{$R_2P(CH_2)_nPR_2$}Rh(1,3-diketonate)][a]

source of parameter	R	change of *n*	Δδ (*r*)	Δδ (*β*)	Δδ (*θ*)	Δδ (*τ*)	ΣΔδ
DFT[b]	Me	2→1	145	24	0	277	446
DFT[b]	Me	2→3	83	50	0	−65	68
DFT[b]	Me	2→4	156	127	1	−59	225
X-ray[c]	Cy	2→1	21	34	35	256	346
X-ray[c]	Ph	2→3	10	33	3	−54	−8
X-ray[c]	Cy	2→4	321	132	−29	−49	375

[a] The Δδ values are obtained by insertion of each parameter value in the respective fitting equations of Figure 4 as evaluated for model compound **13** and forming the difference according to the pair of structures indicated. [b] acac complexes. [c] hfacac complexes.

13 as a function of *τ* (Figure 4d). Indeed, a steep increase of δ(^{103}Rh) is computed for larger values of *τ*.

Explicit values for the four structural parameters discussed above are given in Table 3 for experimental and theoretical structures of selected neutral complexes [(P_2)Rh(hfacac)] and **12**, respectively. Data are taken from X-ray crystallography for **7**, **9** (with R = Ph, Cy) and DFT optimizations for the model complexes **12** (with R = Me). These data can be inserted into the fitting equations of Figure 4 derived from model complex **13** in order to provide chemical shift differences resulting from individual geometric variations between two given structures. The resulting shift differences are summarized in Table 4 for selected pairs of complexes.

The experimental and computational data for the changes in δ(^{103}Rh) of complexes [(P_2)Rh(1,3-diketonate)] resulting from structural variations in the [(P_2)-Rh] fragment are compared in Figure 6. As expected, the absolute values of these differences depend on the substituents at phosphorus and on the applied model approach. Nevertheless, both sets of computational data reproduce the overall trends observed experimentally reasonably well, in view of the inevitable simplifications of the model approach.

When the individual increments are evaluated using structural parameters from single-crystal X-ray diffraction studies, the qualitative agreement between trends in calculated and experimental ^{103}Rh chemical shifts is less satisfactory (Table 4). One possible reason for this discrepancy could be that the conformation of the

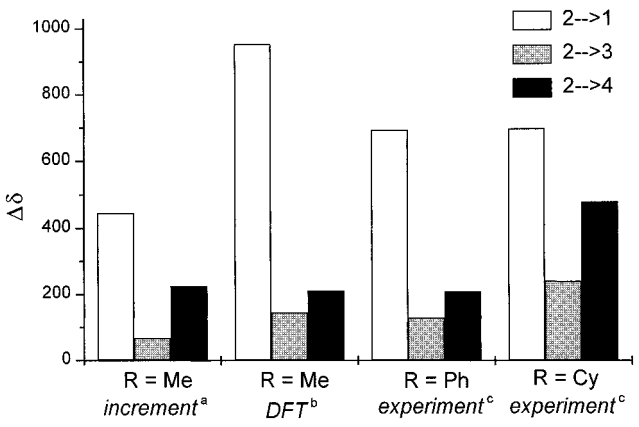

Figure 6. Comparison of calculated and experimental ^{103}Rh chemical shift changes Δδ resulting from variation of the chain length *n* in complexes [{$R_2P(CH_2)_nPR_2$}Rh(1,3-diketonate)]. [a]Sum of the DFT-based Δδ increments (Table 4). [b]Computed change in δ(^{103}Rh) for the model complexes **12a**−**d** (from Table 2). [c]Observed changes in δ(^{103}Rh) for complexes **7a**−**d** and **9a**−**d** in solution (from Table 2).

chelate rings in the solid state structures can be influenced by packing forces and do not necessarily reflect the intrinsic structural parameters of the [(P_2)-Rh] fragment in solution.[13b] On the other hand, this may also reflect the fact that the structural effects on δ(^{103}Rh) are not simply additive. This is already apparent from the fact that the increments based on the DFT structures reproduce the actual, DFT-computed chemical shift trends only qualitatively, not quantitatively (Figure 6).

Although the complexity of the structural influences does not allow the derivation of a general and quantitative increment system at this point, the individual contributions Δδ in Table 4 can help to identify the structural parameter(s) most important for δ(^{103}Rh). Thus, the deshielding of the ^{103}Rh nucleus upon increasing the chelate ring size by elongating the CH_2 backbone is governed simultaneously by the increase of the bite angle *β* and—even more pronounced—the concomitant lengthening of the Rh−P bond (Table 4, entries 2, 3). The decrease of *β* on going from a five- to a four-membered chelate ring is not associated with a further decrease of the Rh−P distance, as this would lead to unacceptably short Rh−P bonds.[49] The deshielding in the four-membered chelate ring is indicated to arise primarily from the tilt angle *τ* as apparent from the large Δδ(*τ*) value in entry 1, Table 4. Although the phosphorus lone pair deviates from the Rh−P axis also in the seven-membered chelate (Figure 5d), the resulting Δδ(*τ*) value is much smaller because of the particular shape of the fitting function in Figure 4d.

(49) The Rh−P bond lengths of more than 90% of rhodium complexes with ligands $R_2P(CH_2)_nPR_2$ located in the Cambridge Structure Database exceed 2.200 Å.

(50) James, B. R.; Mahajan, D. *J. Organomet. Chem.* **1985**, *279*, 31.
(51) (a) Marder, T. B.; Williams, I. D. *J. Chem. Soc., Chem. Commun.* **1987**, 1478. (b) Fornika, R.; Görls, H.; Leitner, W. Unpublished results. (c) Hall, M. C.; Kilbourn, B. T.; Taylor, K. A. *J. Chem. Soc. A* **1970**, 2539. (d) Burch, R. R.; Calabrese, J. C. *J. Am. Chem. Soc.* **1986**, *108*, 5359. (e) Anderson, M. P.; Pignolet, L. H. *Inorg. Chem.* **1981**, *20*, 4101. (f) Jones, R. A.; Real, F. M.; Wilkinson, G.; Galas, A. M. R.; Hursthouse, M. B.; Malik, K. M. A. *J. Chem. Soc., Dalton Trans.* **1980**, 511.
(52) The four-membered rings are puckered in an anti-fashion with respect to each other, as found in the solid state for **14a**; a completely planar arrangement (in D_{2h} symmetry), as essentially observed for solid **14b**, is higher in energy by 0.3 kcal/mol at the BP86/ECP1 level.

Table 5. ^{103}Rh Chemical Shifts and Key Structural Data for Selected Cations $[\{R_2P(CH_2)_nPR_2\}_2Rh]^+$ and $[(R_3P)_4Rh]^+$

cation	*n*	R	$\delta(^{103}Rh)$ (ref)	anion (ref)	P−Rh−P [deg]	P−Rh [Å][a]	twist θ [deg][b]	tilt τ [deg][a,c]
14a	1	Ph	−354[d] (10a)	hfacac (39)	70.80(2)	2.287(1)	0	17.9
14b	1	Cy	−383[d] (10a)	BF_4^- (39)	70.80(2)	2.287(1)	0	17.1
14c	2	Me	−1293[e] (this work)	$C_9H_7^-$ (51a)	85.2(4)	2.282(1)	0	8.2
				$[(cod)RhCl_2]^-$ (51b)	84.0(4)	2.285(1)	0	8.7
			−1345 (DFT, this work)	none (DFT, this work)	84.5	2.316	4.8	7.7
14d	2	Ph	−1171[e] (this work)	ClO_4^- (51c)	82.1(2)/ 83.4(2)	2.306(7)	3.6	7.6
				$[Ag(C_3F_7)]^-$ (51d)	83.5	2.306	7.9	7.8
14e	2	Cy	−1129[e] (this work)	hfacac (39)	84.03(6)/ 82.71(6)	2.334(2)	18.6	9.0
14f	4	Ph		BF_4^- (51e)	90.97(7)/ 89.50(6)	2.329(2)	38	9.2
15a		H	−1223 (DFT, this work)	none (DFT, this work)	90.0	2.304	12.4	4.3
15b		Me		Cl^- (51f)	93.86(5)	2.297(1)	43	9.9
			−516 (DFT, this work)	none (DFT, this work)	93.8	2.337	41.1	8.2

[a] Mean value. [b] The angle between two P_2Rh planes in analogy with Figure 3. [c] See Figure 3 for definition. [d] In CD_2Cl_2. [e] In acetone-d_6. The data reported for cation **14c** in ref 10a, $\delta(^{103}Rh) = -901$, $J(Rh,P) = 98$ Hz, correspond most likely to a Rh(III) species resulting from oxidative addition of CD_2Cl_2 (cf. Marder, T. B.; Fultz, W. C.; Calabrese, J. C.; Harlow, R. L.; Milstein, D. *J. Chem. Soc., Chem. Commun.* **1987**, 1543). [f] One of two independent molecules in the unit cell.

Chart 2. Idealized Coordination Geometries for Cationic and Anionic Complexes of Formula $[Rh(P_2)_2]^{+/-}$

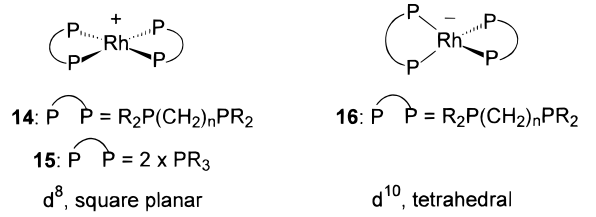

2. Ionic Complexes Containing the $[(P_2)_2Rh]$ Fragment. Our analysis has so far been restricted to neutral four-coordinate complexes of Rh(+I) bearing 1,3-diketonate ligands, and the question arises to what extent the qualitative structure/shift relationships might be affected by the electronic configuration or the coligand. We have therefore extended our studies to coordination compounds of the composition $Rh(P_2)_2$ lacking additional ligands in order to test the generality of our approach. Most of these complexes are d^8 cations, but some can also be reduced to the corresponding d^{10} anions (Chart 2),[53,54] allowing the investigation of the role of the electronic configuration at the metal center without concomitant change of the stabilizing ligand.

Cationic Complexes $[(P_2)_2Rh]^+$. Cationic rhodium complexes with two chelating phosphines represent a large class of coordination compounds with various applications in homogeneous catalysis.[1,50,51e] A large body of crystallographic data for such species is available,[51] and ^{103}Rh chemical shifts have been determined in a number of cases.[10a,h] We have recently synthesized complexes $[(P_2)_2Rh][hfacac]$, which are rare examples of transition metal complexes with noncoordinating hfacac anions.[39] Key structural parameters and $\delta(^{103}Rh)$ values for selected cations $[(P_2)_2Rh]^+$ (**14**) are collected in Table 5.

In analogy with the approach for neutral 1,3-diketonate complexes, the influence of the geometrical arrangement of the $[P_4Rh]^+$ coordination sphere on the chemical shift of the transition metal has been assessed by exploratory calculations for the model compound $[Rh(PH_3)_4]^+$ (**15a**), as well as for $[Rh(PMe_3)_4]^+$ (**15b**) and $[Rh\{Me_2P(CH_2)_2PMe_2\}_2]^+$ (**14c**). For D_2-symmetric **15a**, a slightly twisted structure (12.4° angle between the P−Rh−P planes containing adjacent pairs of phosphines) and a $\delta(^{103}Rh)$ value of −1223 ppm are obtained. Variations of $\delta(^{103}Rh)$ with the structural parameters illustrated in Figure 3 are qualitatively similar to those discussed above for **13**. However, the sensitivity of $\delta(^{103}Rh)$ toward these parameters appears somewhat lower for cationic **15a** than for neutral **13**: for instance, the computed chemical shift derivative with respect to the Rh−P bond length is only ca. 6800 for **15a** compared to more than 10 000 ppm Å^{-1} for **13**.

Exchanging the PH_3 ligands in **15a** with the bulkier PMe_3 (**15b**, D_{2d} symmetry) induces a much larger twist (41.1°), in accord with the experimental value (43°).[51f] This remarkable deviation from the square planar arrangement expected for a d^8 transition metal center results from steric repulsion of the P donor groups.[35,51] Accordingly, the distortion of cations containing two chelating phosphines $R_2P(CH_2)_nPR_2$ increases with the size of R and the chain length *n* as illustrated nicely in the series of compounds **14c**,**d**,**e** and **14a**,**d**,**f**, respectively. The concomitant deshielding represents an important contribution to the ^{103}Rh chemical shift in these cations. For model compound **15a**, the explicit variation of δ with the twist angle θ can be expressed by the fit equation $\delta = 0.300\theta^2 - 1268$, leading to an extreme deshielding of more than 2000 ppm for a hypothetical Rh(+I) cation with two perpendicular $[P_2Rh]$ units.

For **14c** (D_2 symmetry) the optimized $[(P_2)_2Rh]$ moiety is essentially planar (twist angle $\theta = 4.8°$), as found in the solid state,[51b,c] and $\delta(^{103}Rh) = -1345$ is computed in excellent accord with the experimental value of −1293 ppm. In addition, $[Rh(Me_2P(CH_2)PMe_2)_2]^+$ (**14g**) with two four-membered chelate rings has been optimized in C_{2h} symmetry.[52] The computed ^{103}Rh chemical shift of −296 ppm is substantially deshielded with respect to that of **14c**, and the difference $\Delta\delta$ of 1049 ppm arising from the geometrical variation is again in reasonable agreement with the experimental data ob-

(53) Kunin, A. J.; Nanni, E. J.; Eisenberg, R. *Inorg. Chem.* **1985**, *24*, 1852.
(54) Bogdanović, B.; Leitner, W.; Six, C.; Wilczok, U.; Wittmann, K. *Angew. Chem.* **1997**, *109*, 518; *Angew. Chem., Int. Ed. Engl.* **1997**, *36*, 502.

served with the bulkier substituents (**14a**/**14d** $\Delta\delta = 817$, **14b**/**14e** $\Delta\delta = 746$). Like in the case of the neutral 1,3-diketonate complexes, this large effect can be again attributed to the deviation of the Rh−P bond axes from the ideal orientation of the phosphorus lone pair induced by the strained four-membered ring.

Anionic Complexes $[(P_2)_2Rh]^-$. The bis-chelated anions $[\{Ph_2P(CH_2)_nPPh_2\}_2Rh]^-$ ($n = 2$, **16a**; $n = 3$, **16b**) with rhodium in the formal oxidation state (-I) are formed from the corresponding Rh(+I) complexes by electrochemical[53] or chemical reduction.[53,54]

Despite the change in the formal oxidation state, the observed ^{103}Rh chemical shifts of the anions are quite similar to those of the respective cations, e.g., −1018 ppm (**16a**) vs −1171 ppm (**14d**), or −645 ppm (**16b**) vs −593 ppm ($[\{Ph_2P(CH_2)_3PPh_2\}_2Rh]^+$). A geometry optimization starting from the almost planar structure of the d^8 cation **14c** affords an essentially perpendicular arrangement ($\theta = 86.5°$) of the two P−Rh−P planes in the corresponding anion $[\{Me_2P(CH_2)_2PMe_2\}_2Rh]^-$ (**16c**), in accord with the tetrahedral coordination expected for a d^{10} center both on electronic and steric grounds. A ^{103}Rh chemical shift of −1000 ppm is computed for **16c**, consistent with the experimental results for **16a** (−1018 ppm), and this value is indeed in a similar range as theoretical and experimental $\delta(^{103}Rh)$ data of **14c**. Together with the results for the cations discussed above, these data provide a rationalization for the fact that different coordination geometries about Rh are of paramount importance for the ^{103}Rh chemical shifts in tetracoordinate phosphorus containing Rh(+I) cations and Rh(-I) anions and often surpass electronic influences resulting either from inductive effects or from arguments based on formal oxidation states.

Conclusion

Depending on chelate ring size and substitution pattern at phosphorus, the ^{103}Rh chemical shifts of complexes containing the fragment $[(P_2)Rh]$ span a remarkable wide range. Shift differences of over 800 ppm are encountered even for apparently closely related system like $[\{R_2P(CH_2)_nPR_2\}_2Rh(hfacac)]$. Based on a combined experimental and theoretical effort, we have assessed the relative importance of electronic and structural variations for $\delta(^{103}Rh)$. The electronic effects could be separated in isostructural compounds $[\{(p\text{-}XC_6H_4)_2P(CH_2)_4P(p\text{-}XC_6H_4)_2\}Rh(hfacac)]$ as revealed by a linear correlation of $\delta(^{103}Rh)$ with the Hammett σ_P constant of X, indicating a direct inductive influence. This electronic influence leads to variations of the ^{103}Rh chemical shifts not exceeding 80 ppm. In contrast, small variations in the coordination geometry of neutral complexes $[\{R_2P(CH_2)_nPR_2\}Rh(hfacac)]$ were found to induce much larger shift differences. Careful analysis of the individual contributions of changes in key structural parameters of these essentially square planar complexes allowed the rationalization of the observed trends: The relative deshielding of $\delta(^{103}Rh)$ on going to larger chelate-ring sizes ($n > 2$) is mainly induced by the parallel increase of the Rh−P distance and the P−Rh−P angle. In contrast, the large deshielding of the ^{103}Rh nucleus in four-membered chelate rings ($n = 1$) is a consequence of the substantial tilt of the lone pairs at phosphorus away from the Rh−P axis.

The same qualitative relationships hold for cationic complexes with four P donor ligands around a Rh(+I) center. In addition, steric crowding in cationic complexes $[\{R_2P(CH_2)_nPR_2\}_2Rh]^+$ and $[Rh(PR_3)_4]^+$ can induce large deviations from an ideal square planar arrangement expected for a d^8 transition metal center, and the resulting variation in the twist angle of the two $[(P_2)$-Rh] fragments contributes considerably to the relative deshielding of the metal nucleus in complexes with large bite angles and/or bulky substituents at phosphorus. In anionic complexes $[\{R_2P(CH_2)_nPR_2\}_2Rh]^-$ a twist of the two P−Rh−P planes close to the maximum value of 90° is realized, consistent with the expected tetrahedral coordination geometry of a d^{10} Rh(-I) center. This is one of the major reasons for the similarity of the chemical shifts of corresponding $[(P_2)_2Rh]$ cations and anions, despite the different formal oxidation states.

In general terms, we have developed a novel approach to rationalize trends in transition metal chemical shifts based on contributions from discrete variations of geometrical parameters in the coordination sphere. Not surprisingly, the complex interplay of the parameters governing the metal shifts precludes the derivation of a simple quantitative increment system. Nevertheless, our approach provides the basis for a more rational analysis and, thus, for a deeper understanding of structure/shift relationships than possible interpretations in terms of the Ramsey equation. In this respect, our results have important implications for correlations of ^{103}Rh chemical shifts with reactivities and catalytic activities: identification of the electronic and geometric factors governing the metal shifts can help to establish the intrinsic connection between chemical shifts and reactivities. However, the interdependence of the relevant parameters can be quite complex even for apparently closely related compounds, as demonstrated here for example for $[\{R_2P(CH_2)_nPR_2\}_2Rh(hfacac)]$ complexes. Hence, experimentally observed shift/reactivity correlations can generally not be expected to be universally valid and require structural variations to be introduced very systematically, avoiding large simultaneous changes in parameters which have opposite effects on the $\delta(^{103}Rh)$ values.

Acknowledgment. Financial support by the Max-Planck-Society, the Fonds der Chemischen Industrie, and the BMBF is gratefully acknowledged. W.L. wishes to thank U. Beneke, Jena, for preparative assistance, and the Degussa AG for a generous loan of $RhCl_3 \times 3H_2O$. M.B. thanks W. Thiel for his continuous support. We also thank W. von Philipsborn for a preprint of ref 7e. Calculations were performed on Silicon Graphics PowerChallenges (Organisch-chemisches Institut, Universität Zürich) and on IBM RS6000 workstations (C4 cluster, ETH Zürich), as well as on a NEC-SX4 supercomputer (CSCS, Manno, Switzerland).

Supporting Information Available: A listing of analytical data (^{1}H, ^{13}C, ^{31}P, ^{19}F NMR, EI-MS) for ligands **3a**−**e** and complexes **5a**−**e**. This material is available free of charge via the Internet at http://pubs.acs.org. The crystallographic data of complex **9a** have been deposited at the Cambridge Structure Database under the deposition number 101723.

OM980980K